

RESISTIVE BEHAVIOUR OF Nb DIFFUSION-COOLED HOT ELECTRON BOLOMETERS

D. Wilms Floet^{a,1}, J.J.A. Baselmans^a, J.R. Gao^{ab}, and T.M. Klapwijk^a

^aDepartment of Applied Physics and Materials Science Center,
University of Groningen, Nijenborgh 4, 9747 AG Groningen,
The Netherlands

^bSpace Research Organisation of the Netherlands, PO Box 800, 9700 AV Groningen,
The Netherlands

Abstract.

We present a new model for the description of the resistive transition of Nb diffusion-cooled hot electron bolometer mixers. The device is a thin (12 nm) microbridge with a length and width of 220 nm, attached to large Au banks. Heterodyne mixing experiments in a 700 GHz waveguide receiver yield a receiver noise temperature (DSB) of 2200 K at 3.3 K and an IF of 1.4 GHz. We show that the $R(T)$ is an intrinsic property of a superconducting microbridge, connected to normal conducting cooling pads. The essential ingredients of our model are the superconducting proximity effect, charge imbalance and Andreev reflection. Our conclusion is that the resistive transition is not related to the conditions under which the device is operated as a mixer. We propose a mixing mechanism in terms of a normal electronic hotspot of which the length and consequently, the resistance oscillates at the intermediate frequency.

I. Introduction and motivation

The increasing demand for sensitive heterodyne receivers in the terahertz frequency range has largely stimulated the development of hot electron bolometer (HEB) mixers. These devices are being considered as promising candidates for this frequency range, because their noise performance is predicted to not degrade with increasing frequency. Indeed, recent experimental work on HEB mixers has not shown a significant increase of the mixer noise up to 2.5 THz. Also, the intermediate bandwidth of a HEB can be several GHz, which is large enough for many practical applications [1-5].

Several authors have discussed in theoretical models the factors that limit the sensitivity of both diffusion-cooled and phonon-cooled HEBs [6, 7]. They derive expressions for the noise contributions from both Johnson noise and thermal fluctuation noise in terms of the critical temperature T_c of the microbridge, the width of the transition ΔT_c , the radiation coupling factor and the operating temperature T . In these models the $R(T)$ of the microbolometer is represented by a so-called broken-line transition model i.e. $dR/dT = R_N/\Delta T_c$, where R_N is the normal state resistance of the microbridge. It is shown that the noise contribution from thermal fluctuations forms the dominant contribution to the mixer noise and its minimum value does not depend on the width of the transition, as long as ΔT_c is small compared to T_c . Moreover, for a large conversion gain, one desires a narrow transition and a high T_c .

From these points it is clear that in our present understanding of operation of the HEB, the resistive transition plays a crucial role in the sensitivity of the device. On the other hand, a clear physical picture describing the finite transition width of a HEB is not available yet. Here we present a new model which describes the superconducting transition in a Nb diffusion-cooled HEB. We show that the width of the transition is an intrinsic property of a microbridge attached to normal conducting contactpads and also related to the length of the bridge. The paper is organized as follows. In Section II we give an overview of device

¹ electronic mail: wilms@phys.rug.nl

fabrication, DC characterisation and heterodyne performance. In Section III we present a model for the resistive transition in terms of the superconducting proximity effect, charge imbalance and Andreev reflection. The model is compared to measurements of the resistive transition on test-samples. In Section IV we discuss the resistive behaviour of the device when it is operated as a mixer and we propose a mechanism for the mixing process in terms of an oscillating electronic hotspot.

II. Device fabrication and characterization

II.A Device fabrication

We have fabricated Nb diffusion-cooled hot electron bolometers for a 700 GHz waveguide heterodyne receiver by a two step electron beam lithography (EBL) process [8]. First, a 12 nm Nb film is DC sputtered over the whole area of a 200 μm thick fused quartz substrate. The Au cooling pads are defined by EBL using a standard lift-off process. Then, the RF filter and electrical contacts are defined by optical lithography (lift-off). The filter is an in-situ sputtered Nb-Au bilayer. As a last step the bridge between the Au pads is defined by reactive ion etching (RIE). The etch mask (PMMA) is defined using EBL (fine structure) and deep UV exposure (large areas). The R(T) measurements described in Section III are performed on devices where the RF filter is replaced by large electrical contacts (Au).

II.B DC measurements

As a first characterization of the samples, the DC resistance as a function of the temperature is measured using a standard lock-in technique and low current bias conditions (1 μA) in order to avoid self-heating. A typical result for a 220 nm long microbridge is shown in Fig. 1a. Transitions are observed around 6.1 K and 5.4 K. This behaviour was also observed for devices which were produced with optical lithography [9]. Between the two transitions the resistance changes gradually with temperature. It is worth mentioning that R(T) measurements on (large) thin Nb films always show a narrow transition with ΔT_c never larger than 0.1 K.

II.C Heterodyne measurements

We have performed heterodyne measurements with hot and cold loads to determine the DSB receiver noise temperature of the devices. The length and the width of the device under test are both 220 nm and the normal state resistance just above the transition is 24 Ω . We have used a waveguide receiver set-up which was originally designed for Nb SIS mixers around 700 GHz. The device is connected via an isolator to the IF amplifier chain with 80 dB gain at 1.1 GHz and 60 MHz bandwidth. The LO is provided by a carcinotron and is coupled into the mixerblock via a 55 μm thick Mylar beamsplitter.

Fig. 1b shows the IF output powers for hot (295 K) and cold (77 K) input loads as a function of the bias voltage together with unpumped and pumped curves. The measurement is performed at a LO frequency of 735 GHz, a bath temperature of 3.3 K and an IF of 1.1 GHz. The maximum measured Y-factor is 0.22 dB, corresponding to a receiver noise temperature T_{REC} of 2200 K after correction for the beamsplitter loss (0.2 dB). The noise temperature at 4.7 K was 3400 K. No significant variation of the Y-factor is observed when the IF signal is tuned within the gain bandwidth of the amplifier chain (1.1-1.7 GHz), indicating a IF roll-off of at least 1.5 GHz. By calculating the difference in DC power dissipation on a constant resistance line in the pumped and unpumped IV curves we have estimated the coupled LO power to the device. We find a value of 35 ± 5 nW. We have estimated the noise of the mixer

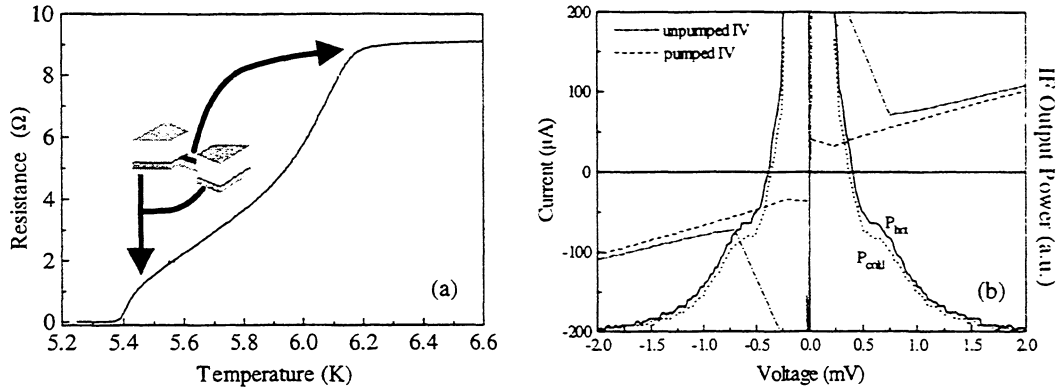


Figure 1 : (a) Resistance as a function of temperature of a Nb HEB. (b) AC IF Output power as a function of bias voltage with hot and cold loads together with pumped and unpumped IV curves. Measurements are carried out at 735 GHz and a bath temperature of 3.3 K. The intermediate frequency is 1.1 GHz.

itself by correcting the receiver noise temperature for the gain and noise contributions of the RF optics and IF amplifier chain using the relation (see also Table 1):

$$T_{\text{rec}} = T_{\text{RF}} + \frac{T_{\text{MIX}}}{G_{\text{RF}}} + \frac{T_{\text{IF}}}{G_{\text{RF}}G_{\text{MIX}}}. \quad (1)$$

with T_{RF} , T_{IF} , and T_{MIX} the noise contributions from the RF-optics, IF amplifier chain and bolometer mixer, respectively, and G_{RF} , G_{IF} and G_{MIX} the corresponding gains. It follows that the mixer noise temperature is 900 K. In the calculation we have not included the mismatch between the mixer and IF amplifier chain. Further improvement of device performance is expected by lowering the bath temperature to 2 K and using a device with a higher resistance i.e. $R_{\text{N}} \sim 50 \Omega$.

	<i>RF Optics</i>	<i>IF Chain</i>	<i>HEB Mixer</i>
Gain	-1.1 dB	80 dB	-24 dB
T_{N}	24 K	3.2 K	-

Table 1: Gain and noise contributions of the RF optics and the amplifier chain.

III. A model for the resistive transition: proximity effect, charge imbalance generation and Andreev reflection

In this section we will present a model which describes the resistive transition. First we will shortly address the observation of two transitions. In the second part of the section we will develop a microscopic model based on charge-imbalance and Andreev reflection, which explains the resistive behaviour at temperatures close to T_{c} .

The observation of two transitions in the $R(T)$ curve of the device is due to the superconducting proximity effect: the parts of the Nb which are covered with Au will have a lower critical temperature (see also Fig. 1a). In previous work [9] we compared the reduced critical temperature with calculations based on a model by Werthamer, but no satisfactory agreement was found. To correctly calculate the actual value of the critical temperature of the thin film as a function the normal metal thickness in N-S sandwiches one has to take into account the electronic properties of both materials and finite transparency of the interface

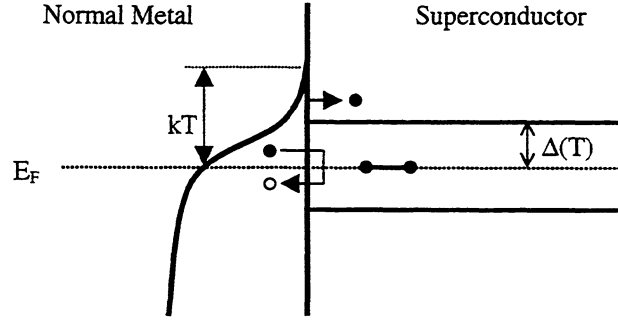


Figure 2: Schematic representation of transport processes near a N-S interface. Electrons with energies $E > \Delta$ are injected as quasi-particles, whereas Andreev reflection occurs for energies $E < \Delta$.

between the two layers, caused by the mismatch in Fermi-velocities in both materials and the possible presence of a potential barrier due to contaminations or interfacial oxides. We have performed measurements and calculations of the critical temperature of Nb-Au bilayers and find good agreement. Details have been described elsewhere [10], but are beyond the scope of this paper.

A second observation is that the resistance is decreasing gradually as a function of temperature in between the two transitions. We show that the observed behaviour can be understood in terms of generation of charge imbalance inside the Nb microbridge. The model allows a description of the $R(T)$ of a fully superconducting microbridge connected to normal electrodes. The resistance is a function of both temperature and bridgelength. Measurements show reasonable agreement with our predictions.

If, at low temperatures, a current is passed through a N-S interface, the normal current is gradually converted into a supercurrent by means of Andreev reflection; an incident electron ($E < \Delta$) is converted into a Cooper pair and a hole is reflected, retracing the path of the electron. This process occurs over a distance ξ , the coherence length of the superconductor and is schematically represented in Fig. 2. However, at temperatures of interest i.e. near T_c , the energy gap Δ becomes smaller than kT and a substantial fraction of the incident electrons enters the superconductor as a quasi-particle, leading to an antisymmetric distribution of the quasi-particles inside the superconductor and consequently to an imbalance of the quasi-particle charge density [11]. To compensate this excess charge, the electrochemical potential of the quasi-particles and Cooper pairs shift in opposite directions, which leads to a measurable (chemical) potential difference given by [12]:

$$\mu_n - \mu_s = \frac{Q^*}{2N_0} . \quad (2)$$

Here Q^* is the excess charge and N_0 the density of states per spin at the Fermi energy. Charge imbalance relaxation can occur via inelastic scattering processes i.e. electron-phonon or electron-electron scattering and its characteristic time, the branch-mixing time, is given by

$$\tau_{Q^*}(T) = \left(\frac{4kT}{\pi\Delta(T)} \right) \tau_{E-E} . \quad (3)$$

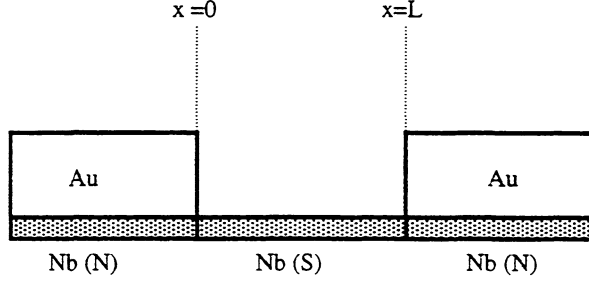


Figure 3: *Schematic cross-section of the HEB as used in the model. The parts of Nb which are covered by Au are normal conducting [Nb (N)], whereas the bridge is a fully superconducting state [Nb(S)].*

Here τ_{E-E} is the inelastic electron scattering time at the Fermi energy. The associated diffusion length is given by

$$\Lambda_{Q^*}(T) = \sqrt{D\tau_{Q^*}(T)}, \quad (4)$$

where D is the electronic diffusion constant.

Let us now consider the situation where a superconducting microbridge of length L is attached to two normal conducting pads (Fig. 3). If the relaxation time τ_{Q^*} is independent of position, this leads to the following differential equation [13]:

$$\frac{d^2(\mu_n(x) - \mu_s)}{dx^2} = \frac{\mu_n(x) - \mu_s}{[\Lambda_{Q^*}(T)]^2}. \quad (5)$$

Assuming that the current is fixed by the source, we use the as boundary condition for $x=0$ and $x=L$:

$$\left. \frac{d(\mu_n(x) - \mu_s)}{dx} \right|_{x=0,L} = \frac{j_n e}{\sigma}. \quad (6)$$

Here σ is the normal state conductivity of the microbridge and j_n is the quasi-particle current which enters the superconductor. With these conditions it is possible to calculate the potential drop across the microbridge, and thus the resistance. We find that

$$R_{\text{bridge}}(T) = \frac{2F^*(T)R_{\text{sq}}}{w} \Lambda_{Q^*}(T) \left[1 - \cosh\left(\frac{L}{\Lambda_{Q^*}(T)}\right) \right] \sinh^{-1}\left(\frac{L}{\Lambda_{Q^*}(T)}\right). \quad (7)$$

R_{sq} is the square resistance of the Nb microbridge and w is the width of the bridge. The factor $F^*(T)$ takes into account that not all current is injected as quasi-particle current, but is partially converted to Cooper pair current by means of Andreev reflection. For $F^*(T)$ we use a result from Blonder, Tinkham and Klapwijk [14] for the N-S interface in the zero-barrier limit. The reason for this is that in our device the actual interface is formed between superconducting and normal conducting Nb (see Fig. 3), so in principle no barrier is expected. Fig. 4 shows the result of the calculation of the normalised resistance as a function of temperature for microbridges with different lengths. In the calculation we have assumed that the inelastic scattering rate is dominated by electron-electron interaction. We have approximated the scattering time by [15]

$$(\tau_E)^{-1} = 10^8 R_{\text{sq}} T. \quad (8)$$

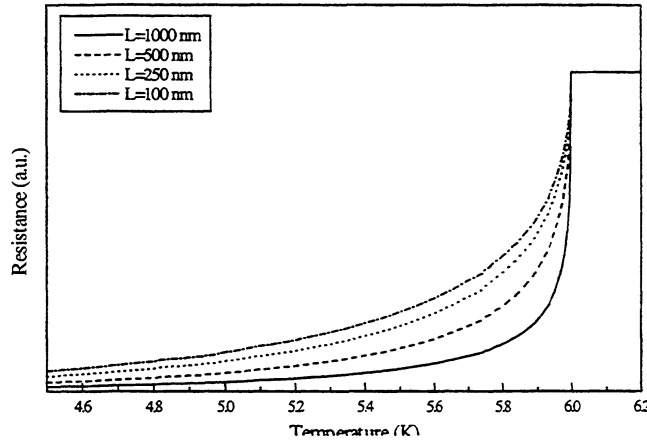


Figure 4: Normalised resistance as a function of temperature for a Nb HEB. The calculation is performed for different lengths of the microbridge.

From the calculation it is clear that the contribution of charge imbalance is depending not only on temperature, but also on the length of the microbridge. Its relative contribution becomes larger with decreasing length.

We have compared the results of the model with $R(T)$ measurements of Nb microbridges with varying length contacted by Au pads. The results are shown in Fig. 5. Fig. 5a shows both measurement and calculation of a 160 nm long microbridge. Reasonable agreement between experiment and model is found, except for temperatures above 5.7 K. Also, below ~ 4.7 K, the Nb under the Au pads is becoming superconducting, so the total resistance drops to zero. Fig. 5a shows the *measured* $R(T)$ of a short (160 nm) and long (1900 nm) bridge. From this figure it is clear that the $R(T)$ depends on the length of the bridge as predicted by our model (see Fig. 4). We have normalised both curves with respect to the normal state resistance and to T_c in order to make the comparison more straightforward. T_c is defined here as the temperature where the resistance has dropped to 90 % of the normal state resistance

Several factors can contribute to the observed differences between model and measurements. In the model it is assumed that there is no spatial variation of the energy gap of the superconductor along the bridge. This assumption is correct, except for temperatures close to T_c , where the coherence length diverges. In this situation it is possible that charge imbalance does not only relax via inelastic scattering, but also via elastic scattering processes [16]. If the last process becomes the dominant one near T_c , one might expect a slower

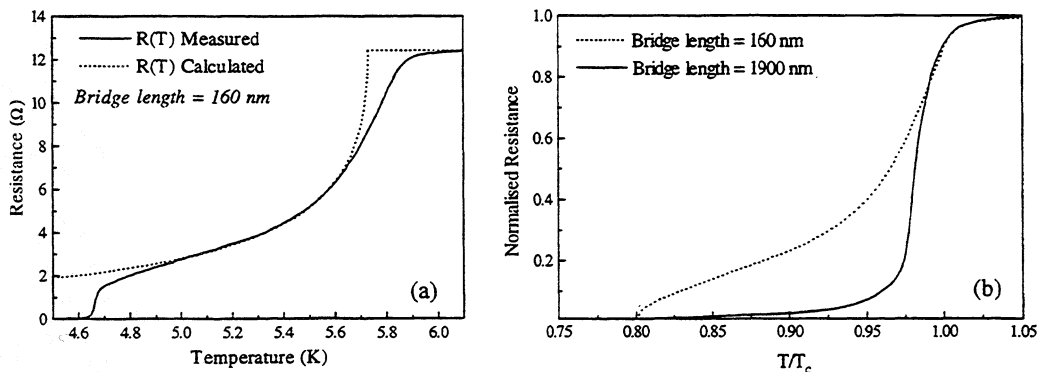


Figure 5: (a) Comparison of the model with experimental data. The figure shows the measured and calculated curve for a 160 nm long microbridge. (b) Experimental $R(T)$ of a long (1900 nm) and short (160 nm) bridge. The data are normalised to T_c and to the normal state resistance.

increase of the resistance. Also, at temperatures close to T_c , we often observe a rounding of the $R(T)$ curve. The physical reason for this is not clear, but superconducting fluctuations can for instance play a role. The rounding makes the estimation of T_c for the calculation somewhat arbitrary. Moreover, in our model it is assumed that the intrinsic superconducting phase transition of Nb can be described by a step-function i.e. $\Delta T_c = 0$. In general we always observe some finite width, although it is usually smaller than 0.1 K.

IV. Resistive behaviour and mixing

The main conclusion from the above presented model is that the resistive transition of a Nb hot electron bolometer is an intrinsic property of a superconducting microbridge connected to normal conducting banks. However, heterodyne mixing experiments are usually performed at temperatures well below the (lowest) transition of the bolometer in order to reduce conversion losses. In this situation the Nb under the Au is superconducting, so charge-imbalance generation does no longer determine the resistance. The high current density inside the microbridge due to LO and DC signals will lead to high dissipation inside the bridge. The Nb/Au banks remain superconducting since the current density there is much lower. It is therefore clear that there exists no direct relation between the DC measured $R(T)$ curve and the resistive behaviour when the device is operated as a mixer.

A naturally resulting question is what the physical state of the microbridge is at its (optimum) operating point i.e. with both DC and LO power dissipation. The Nb/Au banks are superconducting and the microbridge is in a resistive state, thus the situation is in principle analogous to a S-N-S system. It has been shown by Skocpol, Beasley and Tinkham (SBT) that the electrical behaviour of superconducting microbridges at low temperatures can be well described in terms of a localised hotspot, maintained by self-heating [17]. The formation of a hotspot is also the main cause of the observation of hysteresis in the $I(V)$ curve of microbridges at low temperatures. Josephson coupling between the banks (the S-parts) can be important in the description of the $I(V)$ behaviour, but in our case this does not play a role because the coherence length (at low temperature) in the microbridge is much smaller than the bridge length ($\xi \sim 6 \text{ nm} \ll L \sim 200 \text{ nm}$).

The length of the hotspot L_H is directly related to the temperature profile in the microbridge and therefore depends on the amount of dissipated power; larger dissipation will lead to an increase of the size of the hotspot. In the SBT-model equilibrium between the electrons and phonons is assumed. Here we transfer this model to an *electronic hotspot*, in which case the equations are given by:

$$-K \frac{d^2 T}{dx^2} + \frac{c_{el}}{\tau_{e-ph}} (T - T_b) = j^2 \rho \quad (\text{for } |x| < L_H) \quad (9)$$

and

$$-K \frac{d^2 T}{dx^2} + \frac{c_{el}}{\tau_{e-ph}} (T - T_b) = 0 \quad (\text{for } |x| > L_H) \quad (10)$$

Here K is the thermal conductivity of the microbridge and assumed to be the same for superconducting and normal parts and independent of temperature, j is the current density and c_{el} is the electronic heat capacity. In taking this formulation we can use the analytical solutions of SBT at the expense of ignoring the temperature dependence in K and in the heat transfer between electrons and phonons. It is convenient to introduce a thermal healing length $\eta = (D\tau_{e-ph})^{1/2}$, being a measure of the strength of the coupling between the (hot) electrons and the phonons [18]. The relaxation of electrons is dominated by coupling to the phonons if $\eta/L < 1$, whereas diffusion to the normal conducting pads is the dominant relaxation mechanism when $\eta/L > 1$.

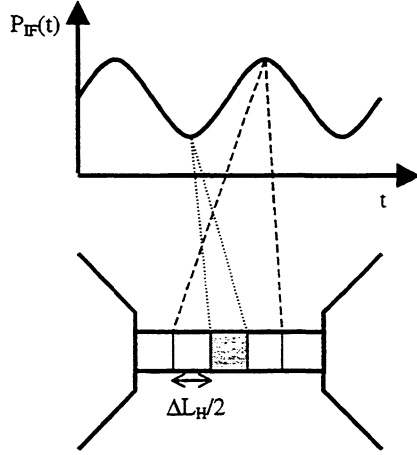


Figure 6: Schematic representation of the mixing process due to the modulation of the size of a hotspot. The grey areas schematically represent the hotspot in case of minimum and maximum power dissipation at the IF frequency. The white parts of the microbridge are superconducting.

In the situation where the device is operated as a mixer, the RF power dissipation is modulated at the intermediate frequency and, as a consequence, the size of the electronic hotspot is modulated. Since the hotspot is a normal (resistive) region, it implies that the resistance of the microbridge is also modulated at the intermediate frequency. Hence, the non-linear response of the device is due to the variation in length of the normal domain with input power. This situation is schematically depicted in Fig. 6. The change of the resistance due to a change in the length of the hotspot (or: change in dissipated power) is given by

$$\Delta R = \left(\frac{R_{sq}}{w} \right) \Delta L_H = \left(\frac{R_{sq}}{w} \right) \left(\frac{dL_H}{dP} \right) \Delta P. \quad (11)$$

Here R_{sq} is the square resistance of the microbridge, L_H the length of the hotspot and P the power dissipated in the hotspot. The voltage responsivity is defined as the change in voltage drop per Watt of absorbed signal power and thus given by

$$S = I \left(\frac{\Delta R}{\Delta P} \right) = I \left(\frac{R_{sq}}{w} \right) \left(\frac{dL_H}{dP} \right), \quad (12)$$

where I is the bias current.

We have calculated $S(V)$ on basis of the heat balance equations given by Eqs. 10 and 11. Fig. 7 shows the result of the calculation. Plotted are the responsivity as a function of bias voltage and the corresponding $I(V)$ curves for along (1000 nm, $\eta/L < 1$) and short (200 nm, $\eta/L > 1$) microbridge. The calculation predicts an increasing sensitivity with decreasing bias voltage, which is in general observed experimentally (Fig. 1b). In practice, however, it is difficult to find a stable bias point on the negative differential part of the $I(V)$, due to relaxation oscillations.

There are a few remarks to be made with respect to the limitations of the calculation. To start with, it is assumed that the absorption of power takes place only in the normal conducting parts. This is true for DC dissipation and RF dissipation, as long as the RF frequency is well below the gap frequency of the superconducting parts (~ 450 GHz). At higher frequencies there is also absorption in the superconducting parts of the bridge and therefore the right term in Eq. 12 is no longer zero, but equals αP_{LO} . Here α is the relative part

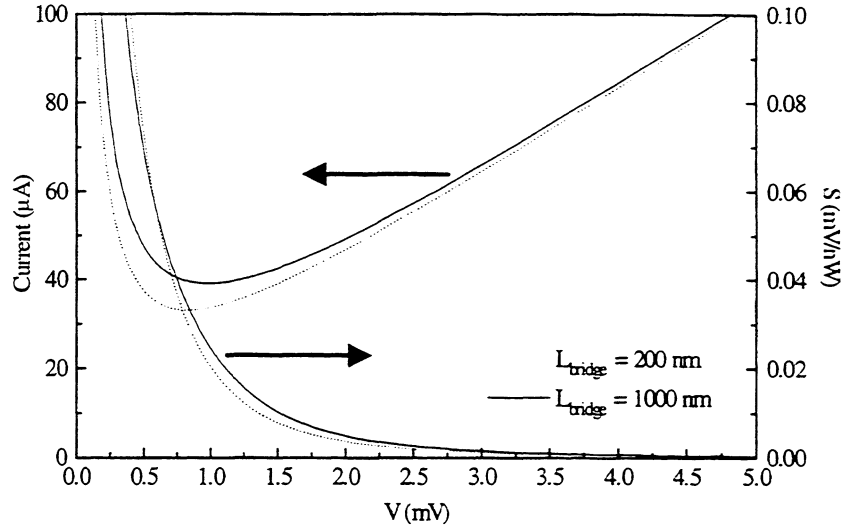


Figure 7: Calculation of the voltage responsivity (see text for definition) as a function of bias voltage together with the corresponding $I(V)$ curve. The calculation is performed in case $L_{\text{bridge}} = 1000 \text{ nm}$ ($\tau/L < 1$, phonon-cooled) and $L_{\text{bridge}} = 200 \text{ nm}$ ($\tau/L > 1$, diffusion-cooled).

of the bridge which is in a superconducting state. Consequently, a term $(1-\alpha)P_{\text{LO}}$ should be added to the right hand side of Eq. 11. Also, the thermal conductivity is taken to be independent of temperature and the same for superconducting and normal state. This is not true in general: the temperature and thermal conductivity are related to each other via the Wiedemann-Franz law and the thermal conductivity is expected to be much lower for the parts which are superconducting. In this case, however, it is not possible to find an analytical solution of the differential equations. Numerical simulations including these factors are in progress. As a last remark we note that in the analysis the N/S interface is sharply defined. Possible effects of non-equilibrium near the interface have not been included. Despite the above limitations of the calculation, we believe that it contains the essential physics.

Conclusions

In conclusion, we have presented a model which describes the resistive transition of Nb diffusion-cooled HEBs. We have shown that it is due to the dissipation in a superconducting microbridge connected to normal conducting heatsinks. We find that by using the concepts of the proximity effect, charge imbalance and Andreev reflection, a satisfactory agreement is found between the model and experimental observations. It follows from the analysis that the (DC measured) resistive transition is not related to the situation where the device is operated in a heterodyne mixing experiment i.e. under the application of DC and LO power. We propose a new mixing mechanism in terms of a (normal conducting) electronic hotspot of which the size oscillates at the intermediate frequency.

Acknowledgements

Helpful ideas, discussions and general assistance from A.A. Golubov, P. de Korte, H. van de Stadt, W.F.M. Ganzevles, E. Miedema and D. Nguyen are acknowledged. This work is financially supported in part by the Stichting voor Technische Wetenschappen and in part by the European Space Agency under contract No. 11738/95/NL/PB.

References

- [1] A. Skalare, W.R. McGrath, B. Bumble, H.G. LeDuc, P.J. Burke, A.A. Verheijen, R.J. Schoelkopf, and D.E. Prober *Appl. Phys. Lett.* 68, 1558 (1996)
- [2] H. Ekström, E. Kollberg, P. Yagoubov, G. Gol'tsman, E. Gershenzon, and S. Yngvesson *Appl. Phys. Lett.* 70, 3296 (1997)
- [3] A. Skalare, W.R. McGrath, B. Bumble, and H.G. LeDuc *IEEE Trans. Appl. Supercond.* 7, 3568 (1997)
- [4] B.S. Karasik, M.C. Gaidis, W.R. McGrath, B. Bumble, and H.G. LeDuc *IEEE Trans. Appl. Supercond.* 7, 3580 (1997)
- [5] P.J. Burke, R.J. Schoelkopf, D.E. Prober, A. Skalare, W.R. McGrath, B. Bumble, and H.G. LeDuc *Appl. Phys. Lett.* 68, 3344 (1996)
- [6] D. E. Prober *Appl. Phys. Lett.* 62, 2119 (1993)
- [7] B.S. Karasik and A.I. Elantiev *Appl. Phys. Lett.* 68, 853 (1996)
- [8] D. Wilms Floet, J.R. Gao, W. Hulshoff, H. van de Stadt, T.M. Klapwijk, and A.K. Suurling *Appl. Supercond.* 1997 401 (1997)
- [9] J.R. Gao, M. E. Glastra, R. H. Heeres, W. Hulshoff, D. Wilms Floet, H. van de Stadt, T.M. Klapwijk, and Th. de Graauw *Proc. 8th Int. Symp. On Space Terahertz Technology*, 36 (1997)
- [10] J. J. A. Baselmans, M. Sc. Thesis, University of Groningen, the Netherlands (1998) and references therein.
- [11] M. Tinkham, *Introduction to Superconductivity*, 2nd edition, McGraw-Hill, Inc. New York, Chapter 11 (1996)
- [12] M. Tinkham and J. Clarke *Phys. Rev. Lett.* 28 1366 (1972)
- [13] M. Stuiyinga, C. L. G. Ham, T. M. Klapwijk, and J. E. Mooij *J. Low Temp. Phys.* 53 (5/6) 633 (1983) and references therein
- [14] G.E. Blonder, M. Tinkham, and T.M. Klapwijk *Phys. Rev. B* 25(7) 4515 (1982)
- [15] P. Santhanam and D. E. Prober *Phys. Rev. B* 29 3733 (1984)
- [16] T. Y. Hsiang and J. Clarke *Phys. Rev. B.* 21 945 (1980)
- [17] W.J. Skocpol, M. R. Beasley, and M. Tinkham *J. Appl. Phys.* 45 (9) 4054 (1974)
- [18] M. Stuiyinga, T. M. Klapwijk, J. E. Mooij, and A. Bezuijen *J. Low Temp. Phys.* 53 (5/6) 673 (1983)